Plant Archives Vol. 20, Supplement 2, 2020 pp. 2586-2593 **e-ISSN:2581-6063 (online), ISSN:0972-5210**

SYNTHESIS AND ULTRASONIC INVESTIGATION OF GRAPHENE OXIDE NANOSUSPENSION WITH WATER

Alok Jain[1], K.C. Juglan[2]*
Department of Physics, School of Chemical Engineering and Physical Sciences Lovely Professional University, Phagwara, 144401, Punjab, India.
Corresponding author e-mail: kc.juglan@lpu.co.in

Abstract

Graphene Oxide (GO) shows remarkable properties in many filed like electronics, sensors, biomedical, thermal conductivity, nanofluids, etc. In this paper, the original Hummers method was used to synthesis GO. Various characterization techniques like FESEM, EDS, FTIR, XRD, and RAMAN were used to verify the conversion of carbon into GO. Suspension of GO in double distilled water with different concentrations was prepared with the help of exhaustive ultrasonication. The stability and presence of GO in the suspension were checked after one week with the help of UV-Vis spectroscopy and the nanoparticle size of GO in the suspension was confirmed with the help of the DLS technique. To calculate the acoustical parameter of the prepared samples ultrasonic velocity, density and viscosity were measured with the help of instruments available. Further, these values were used to calculate parameters like adiabatic compressibility, attenuation, acoustical impedance, etc. Acoustical thermal properties of the prepared sample of Water-GO suspension is reported in this paper.

Keywords: Graphene Oxide; FESEM; XRD; EDS; UV-Vis; Ultrasonic velocity; Density; Viscosity; Relaxation time; Bulk Modulus; Attenuation; Nanosuspension; Adiabatic compressibility

Introduction

Nanosuspension is a colloidal dispersion of nanoparticles that can be controlled by various techniques. The particle size range for solid particles in nanosuspensions is typically smaller than one micron with a median particle size ranging between 100 and 500 nm. (Pardeike *et al.*, 2011) Dispersion of nanoparticle in a base fluid can offer a tremendous change in its properties and because of the extraordinary properties shown by various nanoparticles of metals, metals oxides, ceramic and carbon, it becomes the attraction for many researchers. One fascinating feature of nanofluids is that they have anomalously high thermal conductivity (Rabbani, Mohseni and Rao, 2016), (Sadeghinezhad *et al.*, 2016), (Kharat *et al.*, 2019) which makes nanosuspension strong material for the next generation of coolants for improving the design and performance of thermal management systems. (Torrisi *et al.*, 2012). In recent, applications of nanofluids was also discussed (Ghazvini *et al.,* 2019), (Ahmadi *et al*., 2019a), (Ahmadi *et al*., 2019a), (Ghazvini *et al.,* 2020), (Ahmadi *et al*., 2018), (Ahmadi *et al*., 2019c).

The Brownian motion of nanoparticles in a base liquid is proposed to be one of the major physical mechanisms of the thermal conduction of nanofluids. Therefore; it is significant to investigate the movements of nanoparticles in nanosuspension. Ultrasonication is an accepted technique for the study of such Brownian motion and dispersing aggregated nanoparticles for the preparation of aqueous nanosuspensions (Zhang *et al.*, 2017). Most of the studies have focused on the effect of sonication time on the stability of nanosuspensions and all of them used continuous ultrasonic waves to sonication (Mahbubul *et al.*, 2015). The ultrasonic properties of solid-liquid suspensions in the micrometer size of the particles can cause changes in ultrasonic velocity and ultrasonic attenuation that can affect the thermal conductivity of nanofluids. More specifically, there is an increasing interest mostly in the acoustic properties for acoustic telemetry suspensions via drilling fluids, as well as the rising market for ultrasonic components. Several scientists have researched ultrasonic propagation behavior by suspending solid particles, especially in the nanometre scale of a fluid, with the goal of finding a process that allows vital information to be derived from the behavior of ultrasonic materials, such as particle size, density and mechanical properties of the constituents. Due to their relatively large surface-to-volume ratio, nanoparticles arrested in base liquid substantially expose some new properties that aren't always present in either of the pure components. Hence it is essential to investigate the influence of nanoparticles on the properties of the base liquid in order to effectively anticipate the final properties of the complex fluids.

Graphene is one of the greatest finds of the last decade in terms of many physical and chemical properties. Since its evolution in 2004 range of properties has been reported like: high electron mobility, high thermal conductivity, impermeable to gasses, strongest material ever reported etc. Despite all of these good properties still, there is a number of challenges associated with this material, like industrial-scale productivity, the stability of GO in different available solvents (El-Kady *et al.*, 2012), (Haque *et al.*, 2015), (Lee *et al.*, 2008), (Sheshmani and Fashapoyeh, 2013).

In the present work, we have conducted a study of ultrasonic waves in colloidal dispersion of GO nanoparticles with different concentrations in water to take advantage of the GO properties in the form of nanosuspension. Structural, morphological and fluid-particle interaction studies have been completed and compared. Various acoustical parameters like ultrasonic velocity, density, viscosity were calculated at a temperature range of 298 to 313 K and explained.

Material and Methods

Reagent and chemicals

Graphite powder, sodium nitrate procured from Sigma Aldrich, $KMnO_4$, HCL, H_2SO_4, and Ammonia has been taken from CDH. H_2O_2 has been procured from fisher scientific. All chemicals used in this research were of AR grade and used without additional purification. Throughout all the experiment double distilled water was used.

Methods

Graphene Oxide was prepared using Hummers Method. In short, 3g of graphite powder and 6g of $NaNO_3$ were added in the glass flask containing 120 ml of H_2SO_4 kept on ice bath maintaining 0 ^oC. After continuous stirring of 45 minutes, 12 gm of $KMnO_4$ was added in the suspension very slowly maintaining the temperature below 90 ^oC. The mixture is maintained close to 0 ^oC and kept on continuous stirring for 2 hours. After this mixture is placed in the water bath maintained at 40 ^oC to increase the oxidation reaction. The color of the mixture begins to change from black to brown. Eventually, 30% of the H2O2 is applied to the solution to halt the reaction. The solution is treated with distilled water and sprayed with HCl to remove excess metal ions. The paste is cleaned properly, purified and air-dried with 2 liters of distilled water. Synthesized GO is spread by continuous ultrasonicate in distilled water. Suspension of various concentrations was prepared without adding any further chemical treatment. (Hummers and Offeman, 1958), (Abulizi *et al.*, 2013), (Mahbubul *et al.*, 2015), (Naficy *et al.*, 2014).

Characterization of GO and GO-Water nanosuspension

Nova Nano FESEM 450 with attached EDAX was used for the micro-level imaging of prepared samples. Shimadzu 8400S spectrometer was used for the Fourier transform spectroscopy in range from 400 to 4000 cm^{-1}. Panalytical X'Pret Pro with wavelength 1.54 Å used for the XRD spectra. Confocal Raman Spectrometer Airix STR 500 was used to study the Raman spectrometric studies. Shimadzu UV-1800 spectrometer was used to study the UV-Vis studies of the prepared nanosuspension samples. The average particle size in nanosuspension was verified with the help of Malvern Zetasizer Nano ZS90. The ultrasonic velocity of the prepared samples calculated with the help of Mittal Interferometer M – 81 with a fixed frequency of 2 MHz. Density was calculated with the help of a pycnometer. labman model of LMDV-200 used to calculate the viscosity of all prepared samples.

Result and Discussion

Morphological and elemental analysis

Figure 1 (a) corresponds to the FESEM image of the GO sample at 200000 X magnification. The figure shows how layers of carbon are stacked together in GO.

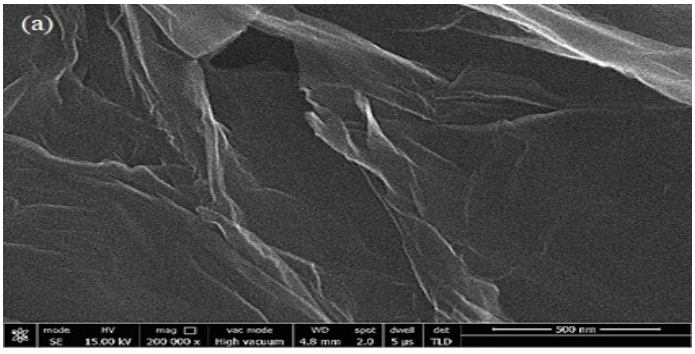

Figure 1: (a) FESEM Image of GO

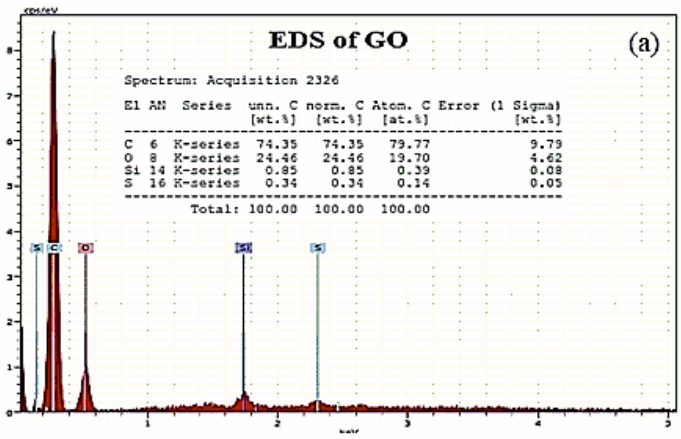

Figure 2: EDS of GO

The EDS graph of GO shows the present content of carbon and oxygen present in the prepared samples which come out to be 74.33% and 24.46% respectively. A large amount of oxygen content present in the prepared sample shows the good oxidation of carbon. It proves the conversion of graphite powder into GO. (Wang, Huang and Huang, 2014), (Roy *et al.*, 2016).

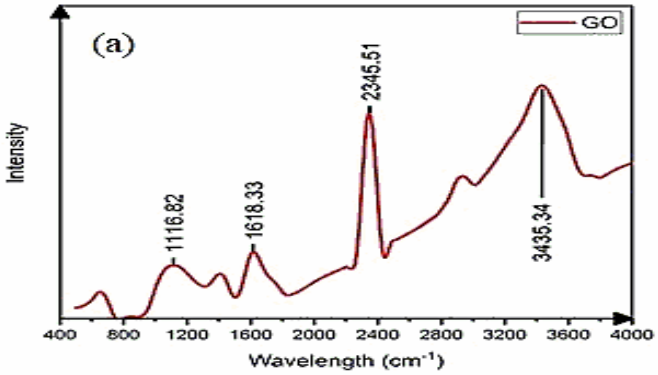

Figure 3: FTIR of GO

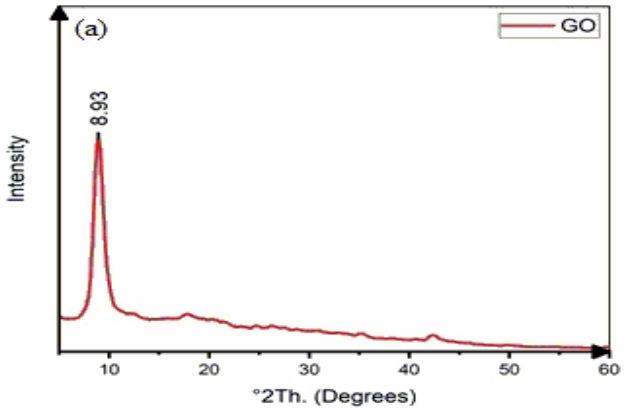

Figure 4: XRD of GO

Figure 3 corresponds to the FTIR spectrum of GO. Peaks at 1116.82 correspond to alkoxy C—O stretching vibration and C—O epoxy stretching vibrations. 1618.33 correspond to C=C Skelton vibrations of the Graphene network, 2345.51 shows the presence of CO_2 (Wang *et al.*, 2017), (Zhu *et al.*, 2015), (Luo *et al.*, 2013). XRD spectra of GO is shown in figure 4. The strong peak at 8.93 contributed toward the (001) crystal plane of GO. The lower value of angle corresponds to the increase in the interplanar distance of the layers of Graphene because of oxygen atoms trapped inside these layers (Liu, Huang and Zhang, 2014), (Liu *et al.*,

2013), (Liu, Yao and Zhou, 2015). Figure 5 shows the Raman spectroscopy graph of the GO samples.

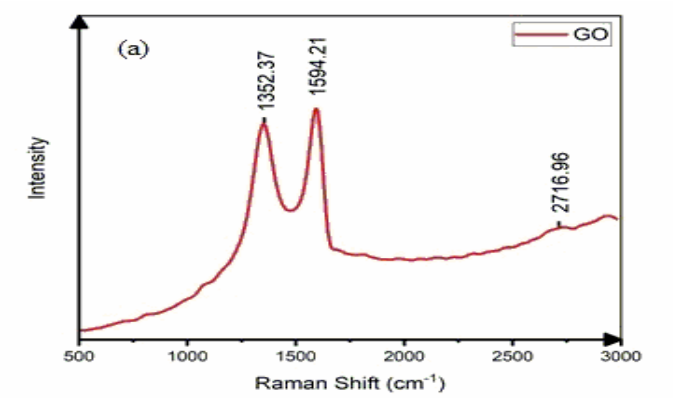

Figure 5: Raman Spectra of GO

The peak at 1352.37 in figure 5 corresponds to defects in the graphene network and the second peak at 1594.21 corresponds to the Graphene Network peak respectively. The intensity ratio of structure defect and Graphene network ratio is I_D/I_G = 0.84 which corresponds to good structure retainment of the graphene network. (Su *et al.*, 2012), (Feng *et al.*, 2016), (Stankovich *et al.*, 2007)

Colloidal Stability analysis

The nanosuspension of water-GO was prepared with the help of extensive ultrasonication. The UV-Vis spectra are shown in figure 6. The peaks at the position of 239 nm confirm the presence of GO in the nanosuspension (Li *et al.*, 2008), ('Preparation of Graphitic Oxide', 1957).The average diameter of GO in water is obtained using a dynamic light scattering (DLS) shown in figure 7.

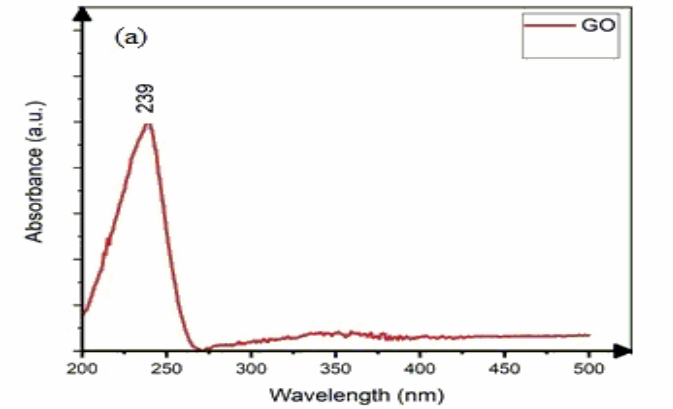

Figure 6: UV Spectra of GO in Water

It is seen that the average size of the GO is in the array of 130 to 155 nm for all 5 prepared samples (Roy *et al.*, 2016), (Ma *et al.*, 2018), (Bao *et al.*, 2011).

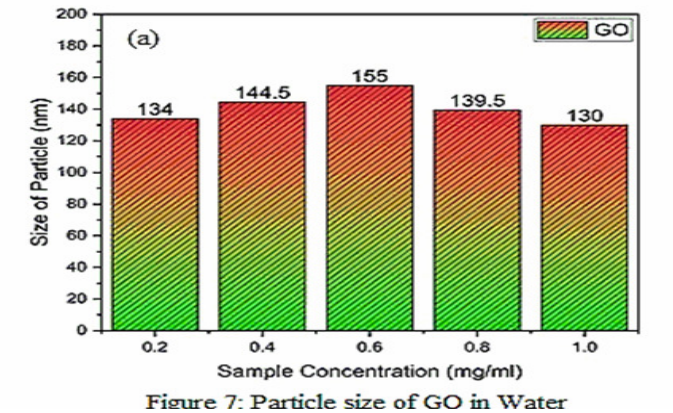

Figure 7: Particle size of GO in Water

With the help of average particle size calculation by DLS, we can categorize the prepared sample as nanosuspension.

Thermoacoustic analysis

Following parameters have been measured in the study.

Ultrasonic Velocity

Ultrasonic velocity is one of the most important parameters for understanding the intraparticle and intermolecular interaction of nanosuspension specimens. The ultrasonic velocity of double distilled water and its solution was measured at four different temperatures (298, 303, 308 and 313 K) and at 1atm pressure. The reading of velocity, density and viscosity were repeated several times for accuracy (Parmar and Banyal, 2005). All measurements for pure water are matched with literature to prevent error. The dissimilarity of ultrasonic velocity with the concentration of nanosuspension and temperature contributes to the understanding of the liquid. Figure 8 indicates the difference of ultrasonic velocity with the concentration of GO in liquid (Parmar and Thakur, 2006) (Thakur *et al.*, 2014)(Thakur, Sharma, Kumar, *et al.*, 2015).

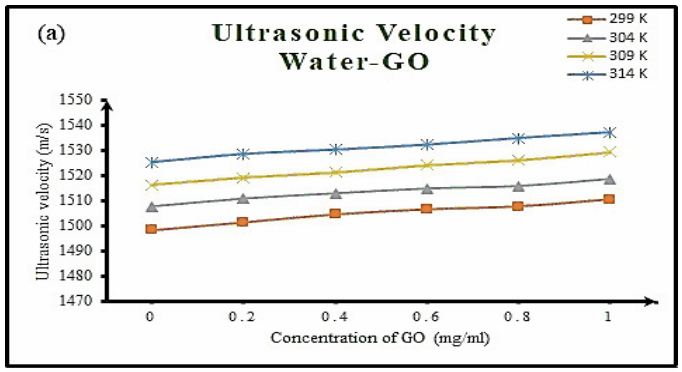

Figure 8: Velocity of sound in Water-GO nanosuspension

Average Velocity(U)				
	299 K	**304 K**	**309 K**	**314 K**
0 (mg/ml)	1498.461	1507.692	1516.15	1525.31
0.2 (mg/ml)	1501.538	1510.846	1519.08	1528.54
0.4 (mg/ml)	1504.615	1512.923	1521.17	1530.23
0.6 (mg/ml)	1506.55	1514.85	1524.05	1532.23
0.8 (mg/ml)	1507.692	1515.846	1526.14	1534.86
1.0 (mg/ml)	1510.46	1518.692	1529.32	1537.15

Ultrasonic velocity grows in water-GO nanosuspension with the upsurge in the concentration of the particles (S. Pathania *et al.*, 2015) (Thakur, Sharma, Meenakshi, *et al.*, 2015). The increment in the ultrasonic velocity has been accredited to the dominance of intramolecular interaction over intermolecular interaction. With the growth in the concentration of the particles, there is a likelihood of an increase in the Brownian motion of nanosuspension and an increase in the surface layer which further helps to increase the ultrasonic velocity. Growth in the temperature of the nanosuspension also increases in the Brownian motion of the fluid molecules which further increase the velocity of the fluid. (Leena, Srinivasan and Prabhaharan, 2015), (Parveen *et al.*, 2009).

Density

As shown in Figure 9, as soon as the GO particle has been added to the pure water, density increases from 997 m / s to 1005 m / s for water-GO nanosuspension at 0.2mg / ml. After this continuous decrease in the density of the prepared nanosuspension with a rise in the concentration of the particles can be seen (S. K. Pathania *et al.*, 2015) (Sonika and Thakur, 2015) (Thakur, Sharma and Bala, 2016) (Ramesh Thakur, 2016) (Thakur, 2016) (Thakur, 2016) (Sharma and Thakur, 2017)

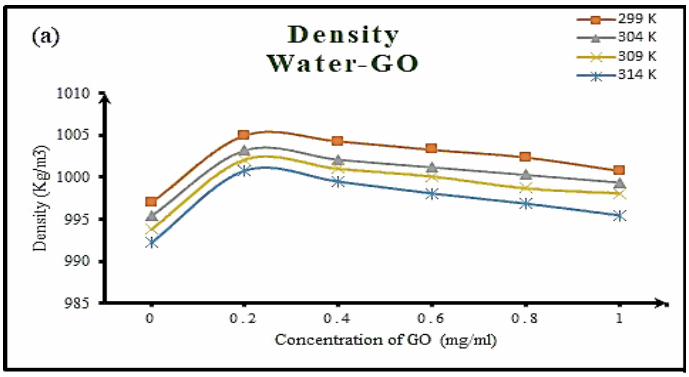

Figure 9: Density of Water-GO Nanosuspension

Density(ρ)				
	299 K	304 K	309 K	314 K
0 (mg/ml)	997	995.4	993.8	992.2
0.2 (mg/ml)	1005	1003.2	1002.1	1000.8
0.4 (mg/ml)	1004.3	1002.1	1001	999.5
0.6 (mg/ml)	1003.3	1001.2	1000.1	998.1
0.8 (mg/ml)	1002.4	1000.3	998.7	996.9
1.0 (mg/ml)	1000.8	999.4	998.1	995.5

This is due to an increase in intramolecular interaction rather than intermolecular interaction. Density drops with the rise in the temperature of nanosuspensions (Vajjha, Das and Mahagaonkar, 2009), (Ranjini, Mahalingam and Jeevaraj, 2012).

Viscosity

Viscosity of the water-GO nanosuspension declines with a rise in temperature due to the increase in the Brownian motion of the water molecules. The increase in the temperature flow of nanosuspension also becomes easy. Viscosity also increases slightly with an increase of particle loading in nanosuspension, which is due to a restriction in the flow produced by GO nanoparticles**.** These particles get tangled with each other to restrict the flow of liquids (Rabbani, Mohseni and Rao, 2016), (Parveen *et al.*, 2009) (Thakur and Sharma, 2017) (Sharma *et al.*, 2017) (Sharma and Thakur, 2018) (Sonika *et al.*, 2018).

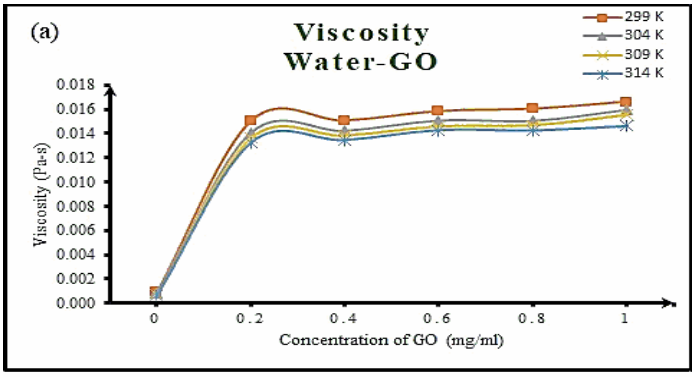

Figure 10: Viscosity of Water-GO nanosuspension

Viscosity(η)				
	299 K	304 K	309 K	314 K
0 (mg/ml)	0.00089	0.000797	0.000719	0.000653
0.2 (mg/ml)	0.015014	0.014089	0.0136	0.013263
0.4 (mg/ml)	0.015044	0.01425	0.01382	0.01346
0.6 (mg/ml)	0.015822	0.0151	0.014575	0.014289
0.8 (mg/ml)	0.01602	0.015075	0.014675	0.01426
1.0 (mg/ml)	0.016612	0.015978	0.015528	0.01462

Adiabatic Compressibility

Figure 11 shows a decrease in adiabatic compressibility with a rise in the concentration of the particles. Decreased adiabatic compressibility with increased concentration of the particles promotes fluid-particle interaction. In addition, adiabatic compressibility also decreases with an increase in system temperature (Kumar *et al.*, 2016), (Hemalatha, Prabhakaran and Pratibha Nalini, 2011) (Chakraborty *et al.*, 2018) (Kaur *et al.*, 2018) (Kaur, Kailash C. Juglan and Kumar, 2017).

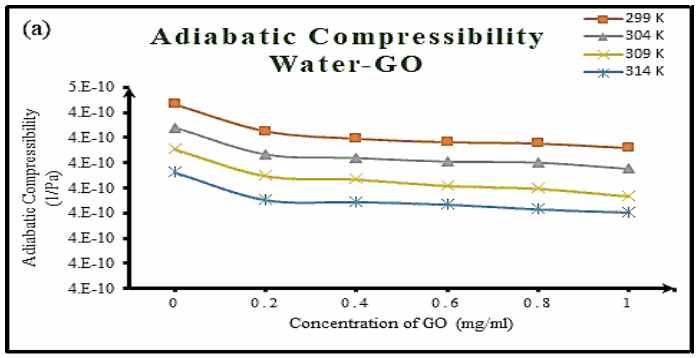

Figure 11: Adiabatic compressibility of Water-GO nanosuspension

Adiabatic Compressibility(β)				
	299 K	304 K	309 K	314 K
0 (mg/ml)	4.47E-10	4.42E-10	4.38E-10	4.33E-10
0.2 (mg/ml)	4.41E-10	4.37E-10	4.32E-10	4.28E-10
0.4 (mg/ml)	4.40E-10	4.36E-10	4.32E-10	4.27E-10
0.6 (mg/ml)	4.39E-10	4.35E-10	4.30E-10	4.27E-10
0.8 (mg/ml)	4.39E-10	4.35E-10	4.30E-10	4.26E-10
1.0 (mg/ml)	4.38E-10	4.34E-10	4.28E-10	4.25E-10

Acoustic Impedance

Figure 12 shows an increase in the value of acoustic impedance in nanosuspension with an increase in the number of particles. Increased values of acoustic impedance suggest that there is a significant collaboration between nanoparticles and liquid which can affect the structural arrangement. On the other side, the acoustic impedance for nanosuspensions increases with an uprise in temperature that can be due to an increase in the Brownian motion of base fluid molecules.

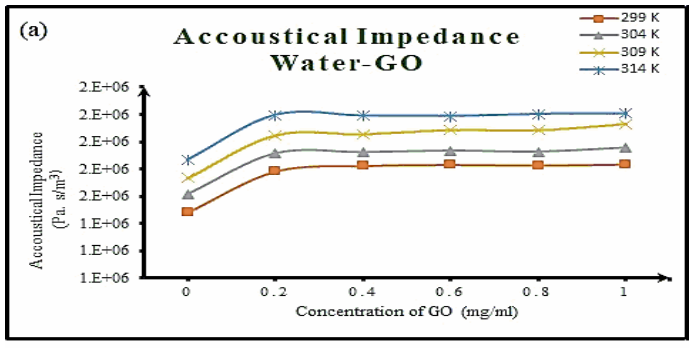

Figure 12: Accoustical Impedance of Water-GO nanosuspension

Increasing particle-fluid interactions at lower concentrations increase the intermolecular gap which provides resistance to the propagation of ultrasonic waves. (Khushboo *et al.*, 2016; Gupta and Sharma, 2014; Kaur and Kumar, 2017; Manon *et al.*, 2017)

Acoustical impedance(Z)				
	299 K	304 K	309 K	314 K
0 (mg/ml)	1493966.2	1500756.9	1506749.9	1513412.6
0.2 (mg/ml)	1509046.2	1515680.9	1522270.1	1529762.8
0.4 (mg/ml)	1511085.2	1516100.2	1522691.2	1529464.9
0.6 (mg/ml)	1511521.6	1516667.8	1524202.4	1529318.8
0.8 (mg/ml)	1511310.8	1516300.9	1524156	1530101.9
1.0 (mg/ml)	1511668.4	1517781.1	1526414.3	1530232.8

Ultrasonic attenuation

Figure 13 demonstrates the attenuation of ultrasound waves when going through prepared nanosuspensions. Ultrasonic attenuation increases dramatically with the addition of nanoparticles to the base fluid because the network of these particles can block most of the ultrasonic waves from reaching the other end.

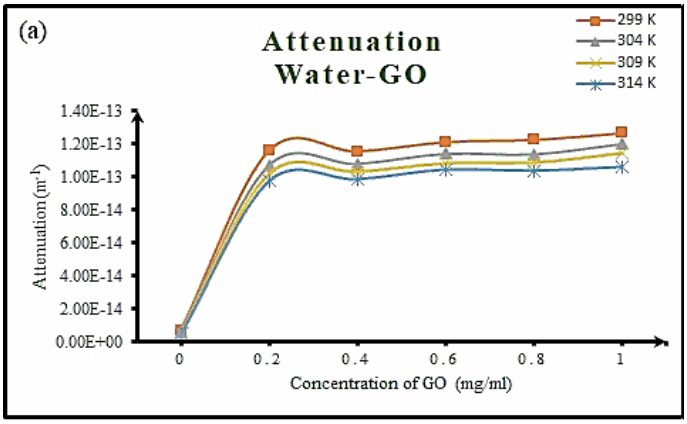

Figure 13: Attenuation of Water-GO nanosuspension

Attenuation (α/f2)				
	299 K	304 K	309 K	314 K
0 (mg/ml)	6.98E-15	6.14E-15	5.46E-15	4.88E-15
0.2 (mg/ml)	1.16E-13	1.07E-13	1.02E-13	9.76E-14
0.4 (mg/ml)	1.16E-13	1.08E-13	1.03E-13	9.88E-14
0.6 (mg/ml)	1.21E-13	1.14E-13	1.08E-13	1.05E-13
0.8 (mg/ml)	1.23E-13	1.14E-13	1.09E-13	1.04E-13
1.0 (mg/ml)	1.27E-13	1.20E-13	1.14E-13	1.06E-13

Therefore, with the rise in the density of the samples, the attenuation decreases only marginally. Moreover, the reliance on attenuation on temperature can be seen in all other nanosuspension preparations. It can be seen that as the temperature rises, the magnitude of the attenuation declines because of the rate of Brownian motion increases in the base liquid (Kaur and Juglan, 2015; Tajik *et al.*, 2012).

Bulk Modulus

It can be described as the resistance of the liquid or fluid to the stress applied. In Figure 14, the bulk modulus tends to increases for the water-GO nanosuspension with the growth in the count of the particles in nanosuspension. Bulk modulus also increases with increased temperature.

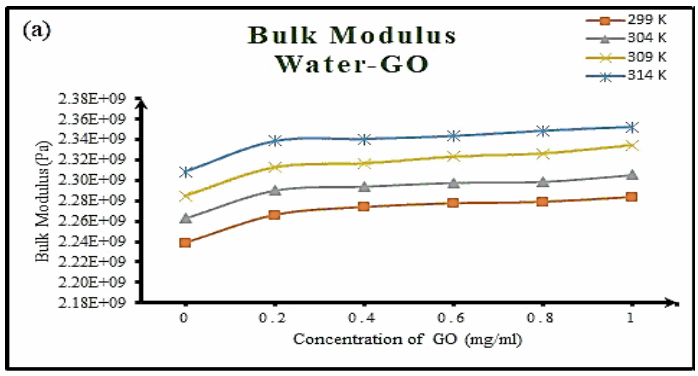

Figure 14: Bulk Modulus of Water-GO nanosuspension

Bulk Modulus(K)				
	299 K	304 K	309 K	314 K
0 (mg/ml)	2.239E+09	2.263E+09	2.284E+09	2.308E+09
0.2 (mg/ml)	2.266E+09	2.29E+09	2.312E+09	2.338E+09
0.4 (mg/ml)	2.274E+09	2.294E+09	2.316E+09	2.34E+09
0.6 (mg/ml)	2.277E+09	2.298E+09	2.323E+09	2.343E+09
0.8 (mg/ml)	2.279E+09	2.298E+09	2.326E+09	2.348E+09
1.0 (mg/ml)	2.283E+09	2.305E+09	2.334E+09	2.352E+09

An increase in bulk modulus or reduction in compressibility attributes to the fact that robust, collaboration forces act between molecules of the base fluid after the dispersion of GO nanoparticles in water (Ayachit *et al.*, 2007), (Elangovan and Mullainathan, 2013).

Relaxation Time

Figure 15 indicates the relaxation time of the water-GO nanosuspension. Relaxation time is the duration of molecular re-arrangement during the propagation of ultrasonic waves from the fluid. It can be seen clearly in Figure 15 that relaxation time rises from $5.3 \times 10^{-12}s$ to 8.83×10^{-12}s purely because of the introduction of GO nanoparticles to pure water.

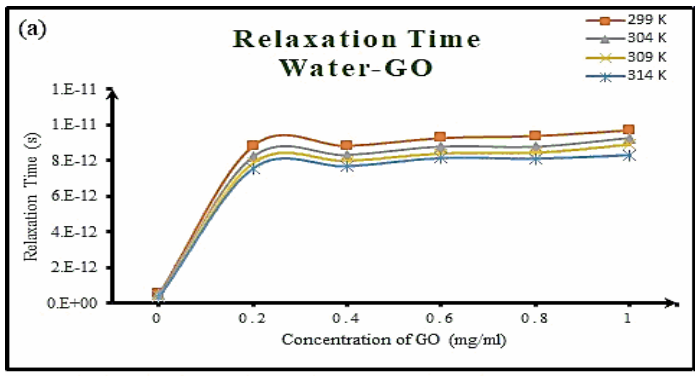

Figure 15: Ralaxation time of Water-GO nanosuspension

Relaxation Time(τ)				
	299 K	304 K	309 K	314 K
0 (mg/ml)	5.30E-13	4.70E-13	4.20E-13	3.77E-13
0.2 (mg/ml)	8.83E-12	8.20E-12	7.84E-12	7.56E-12
0.4 (mg/ml)	8.82E-12	8.28E-12	7.96E-12	7.67E-12
0.6 (mg/ml)	9.26E-12	8.76E-12	8.37E-12	8.13E-12
0.8 (mg/ml)	9.37E-12	8.74E-12	8.41E-12	8.10E-12
1.0 (mg/ml)	9.70E-12	9.24E-12	8.87E-12	8.29E-12

In addition, a slight increase in relaxation time is seen in nanosuspensions. Relaxation time declines with an increase in temperature as the Brownian motion of water molecules rise with an increase in temperature (Elangovan

and Mullainathan, 2013), (Naik, 2015)(Parmar, Dhiman and Thakur, 2002).

Intermolecular free length

It can be clearly understood from Figure 16 that the intermolecular free length is a function of temperature. As the temperature rises, the free intermolecular free length reduces as the relaxation period increases.

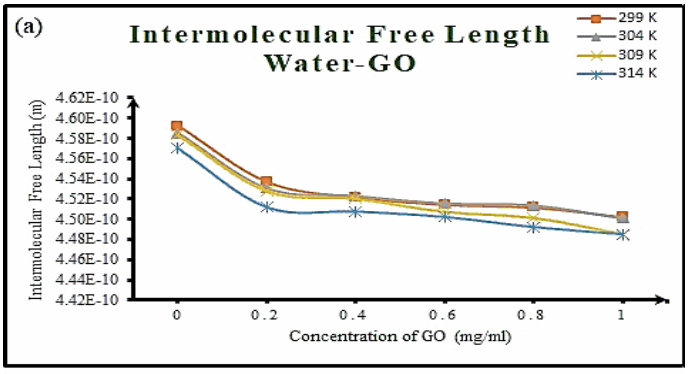

Figure 16: Intermolecular free length of Water-GO nanosuspension

Intermolecular Free Length (Lf)				
	299 K	304 K	309 K	314 K
0 (mg/ml)	4.59E-10	4.59E-10	4.58E-10	4.57E-10
0.2 (mg/ml)	4.54E-10	4.53E-10	4.53E-10	4.51E-10
0.4 (mg/ml)	4.52E-10	4.52E-10	4.52E-10	4.51E-10
0.6 (mg/ml)	4.51E-10	4.52E-10	4.51E-10	4.50E-10
0.8 (mg/ml)	4.51E-10	4.51E-10	4.50E-10	4.49E-10
1.0 (mg/ml)	4.50E-10	4.50E-10	4.49E-10	4.49E-10

Therefore, the intermolecular free length falls with a rise in the density of nanoparticles in the base liquid. This activity is the result of liquid and particle interactions in nanosuspension (Khushboo *et al.*, 2016), (Gupta, Sharma and Sharma, 2014).

Conclusion

Graphene oxide and reduced graphene oxide were prepared using the Original Hummer Method. Various characterization techniques including FESEM, XRD, FTIR, EDS, and RAMAN have been used to confirm the conversion of GO. Prepared GO powder was dispersed directly into distilled water using an ultrasonic technique. Samples with varying densities have been prepared for ultrasonic studies. The ultrasound analysis of Water-GO nanosuspension reveals the superiority of intramolecular interaction over intermolecular interaction. Ultrasound velocity increases with an increase in concentration due to a decrease in the intermolecular free length of the nanosuspension molecules. The density of both nanosuspension reduces and the viscosity rises with a rise in the concentration of GO particles. Adiabatic compressibility, intermolecular free length, decreases with increased concentration. This decrease in acoustic parameters indicates that there is a weak interaction between the molecules of the base fluid and GO nanoparticles. Acoustic impedance, bulk modulus, attenuation and relaxation time show an increase in the concentration of GO, suggesting the lack of a complex formation in the nanosuspension.

Acknowledgments

The writer would like to thank the Lovely Professional University for providing the necessary laboratory facilities at the Department of Physics. The writer is also thankful to MNIT Jaipur for support in characterization.

References

'Preparation of Graphitic Oxide' (1957): 208(1937): 1937

Abulizi, A. *et al.* (2013) 'Vitamin C Is an Ideal Substitute for Hydrazine in the Reduction of Graphene Oxide Suspensions', The Journal of Physical Chemistry C, 4(3): 6426–6432.

Ahmadi, M.H.; Ramezanizadeh, M.; Nazari, M.A.L.; Giulio. Kumar, R. Jilte, R. (2018). Applications of nanofluids in geothermal: A review, Mathematical Modelling of Engineering Problems, 5(4): 281-285.

Ahmadi, M.H.; Kumar, R.; Mohseni-Gharyehsafa, B.; Ghazvini, M.; Goodarzi, M. and Jilte, R.D. (2019a). Comparing Various Machine Learning Approaches in Modeling the Dynamic Viscosity of CuO/Water Nanofluid, Journal of Thermal Analysis and Calorimetry.

Ahmadi, M.H.; Mohseni-Gharyehsafa, B.; Farzaneh-Gord, M.; Kumar, R.; Jilte, R. and Chau, K.W. (2019b). Applicability of connectionist methods to predict dynamic viscosity of Ag/water nanofluid by using ANN-MLP, MARS and MPR algorithms, Engineering Applications of Computational Fluid Mechanics, 13(1): 220-228.

Ahmadi, M.H.; Sadeghzadeh, M.; Maddah, H.; Solouk, A.; Kumar, R. and Chau, K.W. (2019). Precise smart model for estimating dynamic viscosity of SiO_2/ethylene glycol–water nanofluid, Engineering Applications of Computational Fluid Mechanics, 13(1): 1095-1105.

Ayachit, N.H. *et al.* (2007) 'Thermodynamic and acoustical parameters of some nematic liquid crystals', Journal of Molecular Liquids, 133(1–3): 134–138

Bao, H. *et al.* (2011) 'Chitosan-functionalized graphene oxide as a nanocarrier for drug and gene delivery', Small, 7(11): 1569–1578.

Chakraborty, N. *et al.* (2018) 'Acoustic and thermodynamic study of D-Panthenol in aqueous solutions of glycol at different temperatures', Journal of Chemical Thermodynamics, 126: 137–146.

Elangovan, S. and Mullainathan, S. (2013) 'Ultrasonic studies of intermolecular interaction in binary mixture of n-methyl formate with 1-propanol at various temperatures', Indian Journal of Physics, 87(7): 659–664.

El-Kady, M.F. *et al.* (2012) 'Laser scribing of high-performance and flexible graphene-based electrochemical capacitors', Science, 335(6074): 1326–1330.

Feng, W. *et al.* (2016) 'Reduced graphene oxide decorated with in-situ growing ZnO nanocrystals: Facile synthesis and enhanced microwave absorption properties', Carbon. Elsevier Ltd, 108: 52–60.

Ghazvini M, Maddah H, Peymanfar R, Ahmadi M.H, Kumar R (2020) Experimental evaluation and artificial neural network modeling of Thermal Conductivity of water based nanofluid containing Magnetic copper nanoparticles, Physica A: Statistical Mechanics and its Applications, (In press) 10.1016/j.physa.2019.124127

Ghazvini, M.; Maddah, H.; Peymanfar, R.; Ahmadi, M.H. and Kumar, R. (2020). Experimental evaluation and artificial neural network modeling of thermal conductivity of water based nanofluid containing

magnetic copper nanoparticles. Physica A: Statistical Mechanics and its Applications, 124127.

Gupta, V.; Sharma, A. K. and Sharma, M. (2014) 'Ultrasonic investigation of molecular interaction in aqueous glycerol and aqueous ethylene glycol solution', Journal of Chemical and Pharmaceutical Research, 6(1): 714–720.

Haque, A.K.M.M. *et al.* (2015) 'An experimental study on thermal characteristics of nanofluid with graphene and multi-wall carbon nanotubes', 3202–3210.

Hemalatha, J.; Prabhakaran, T. and Pratibha Nalini, R. (2011) 'A comparative study on particle-fluid interactions in micro and nanofluids of aluminium oxide', Microfluidics and Nanofluidics, 10(2): 263–270.

Hummers, W.S. and Offeman, R. E. (1958) 'Preparation of Graphitic Oxide', Journal of the American Chemical Society, 80(6): 1339.

Kaur, K. and Juglan, K.C.C. (2015) 'Studies of molecular interaction in the binary mixture of chloroform and methanol by using ultrasonic technique', Der Pharma Chemica, 7(2): 160–167.

Kaur, K. *et al.* (2018). Volumetric and ultrasonic studies on interactions of ethylene glycol, diethylene glycol and triethylene glycol in aqueous solutions of glycerol at temperatures T=(293.15 K–308.15) K', Journal of Chemical Thermodynamics, 125: 93–106.

Kaur, K.; Juglan, K.C. and Kumar, H. (2017) 'Thermo-acoustical molecular interaction study in binary mixtures of glycerol and ethylene glycol', AIP Conference Proceedings, 1860.

Kaur, K.; Juglan, Kailash C. and Kumar, H. (2017) 'Investigation on Temperature-Dependent Volumetric and Acoustical Properties of Homologous Series of Glycols in Aqueous Sorbitol Solutions', Journal of Chemical and Engineering Data, 62(11): 3769–3782.

Kharat, P.B. *et al.* (2019) 'Exploration of thermoacoustics behavior of water based nickel ferrite nanofluids by ultrasonic velocity method', Journal of Materials Science: Materials in Electronics. Springer US, 30(7): 6564–6574.

Khushboo *et al.* (2016) 'Thermodynamic and acoustical study of zinc oxide-nematic liquid crystals mixtures', Journal of Molecular Liquids, 214(February): 145–148.

Kumar, H. *et al.* (2016) 'Study of thermodynamic properties of sodium dodecyl sulphate in aqueous solutions of alkoxyalkanols at different temperatures', Journal of Molecular Liquids. Elsevier B.V.; 221, 526–534.

Lee, C. *et al.* (2008) 'Measurement of the elastic properties and intrinsic strength of monolayer graphene', Science, 321(5887): 385–388.

Leena, M.; Srinivasan, S. and Prabhaharan, M. (2015) 'Evaluation of acoustical parameters and thermal conductivity of TiO2-ethylene glycol nanofluid using ultrasonic velocity measurements', Nanotechnology Reviews, 4(5): 449–456.

Li, D. *et al.* (2008) 'Processable aqueous dispersions of graphene nanosheets', Nature Nanotechnology, 3(2): 101–105.

Liu, J. *et al.* (2013) 'A green approach to the synthesis of high-quality graphene oxide flakes via electrochemical exfoliation of pencil core', RSC Advances, 3(29): 11745.

Liu, P.; Huang, Y. and Zhang, X. (2014) 'Superparamagnetic NiFe2O4 particles on poly(3,4-ethylenedioxythiophene)-graphene: Synthesis, characterization and their excellent microwave absorption properties', Composites Science and Technology. Elsevier Ltd, 95, 107–113.

Liu, P.; Yao, Z. and Zhou, J. (2015) 'Preparation of reduced graphene oxide/Ni0.4Zn0.4Co0.2Fe_2O_4 nanocomposites and their excellent microwave absorption properties', Ceramics International. Elsevier, 41(10): 13409–13416.

Luo, Z. *et al.* (2013) 'Effects of graphene reduction degree on capacitive performances of graphene/PANI composites', Synthetic Metals. Elsevier B.V.; 175, 88–96.

Ma, J. *et al.* (2018) 'Solubility study on the surfactants functionalized reduced graphene oxide', Colloids and Surfaces A: Physicochemical and Engineering Aspects. Elsevier B.V.; 538, 79–85.

Mahbubul, I. M. *et al.* (2015) 'Effective ultrasonication process for better colloidal dispersion of nanofluid', Ultrasonics Sonochemistry. Elsevier B.V.; 26: 361–369.

Manon, P. *et al.* (2017) 'Intermolecular interaction studies of glyphosate with water', AIP Conference Proceedings, 1860: 1–8.

Naficy, S. *et al.* (2014) 'Graphene oxide dispersions: Tuning rheology to enable fabrication', Materials Horizons, 1(3): 326–331.

Naik, A. B. (2015) 'Densities, viscosities, speed of sound and some acoustical parameter studies of substituted pyrazoline compounds at different temperatures', Indian Journal of Pure and Applied Physics, 53(1): 27–34.

Pardeike, J. *et al.* (2011) 'Nanosuspensions as advanced printing ink for accurate dosing of poorly soluble drugs in personalized medicines', International Journal of Pharmaceutics. Elsevier B.V.; 420(1): pp. 93–100

Parmar, M.L. and Banyal, D.S. (2005). Effect of temperature on the partial molar volumes of some bivalent transition metal nitrates and magnesium nitrate in DMF + water mixtures', Indian Journal of Chemistry - Section A Inorganic, Physical, Theoretical and Analytical Chemistry, 44(8): 1582–1588.

Parmar, M.L. and Thakur, R.C. (2006). Effect of temperature on the partial molar volumes of some divalent transition metal sulphates and magnesium sulphate in the water-rich region of aqueous mixtures of ethylene glycol', Journal of Molecular Liquids, 128(1–3): 85–89.

Parmar, M.L.; Dhiman, D.K. and Thakur, R.C. (2002) 'Jc', pp. 2032–2038.

Parveen, S. *et al.* (2009) 'Ultrasonic velocity, density, viscosity and their excess parameters of the binary mixtures of tetrahydrofuran with methanol and o-cresol at varying temperatures', Applied Acoustics, 70(3): 507–513.

Pathania, S. *et al.* (2015). Influence of bovine serum albumin (BSA) on micellization behaviour of sodiumdodecylsulphate (SDS) in aqueous rich mixtures of dimethylsulfoxide at different, Researchgate.Net, (January).

Pathania, S.K. *et al.* (2015). A comparative study of interactions between protein (Lysozyme) and ionic surfactants (SDS, CTAB) in aqueous rich mixtures of DMSO at different temperatures, Research Journal of Pharmaceutical, Biological and Chemical Sciences, 6(1): 721–729.

Rabbani, M.; Mohseni, E. and Rao, M. (2016) 'Effect of particle size and viscosity on thermal conductivity

enhancement of graphene oxide nano fl uid ☆', International Communications in Heat and Mass Transfer. Elsevier Ltd, 76: 308–315.

Ramesh Thakur, R.S. and B. S. (2016) 'Effect of temperature on the volumetric and viscometric properties of polyols in aqueous solutions', Journal of Molecular Liquids, 223(1): 1192–1196.

Ranjini, K.; Mahalingam, T. and Jeevaraj, A.K.S. (2012) 'Ultrasonic Studies on Zinc Oxide Nanofluids', (May 2014).

Roy, I. *et al*. (2016) 'Synthesis and characterization of graphene from waste dry cell battery for electronic applications', RSC Adv.; 6(13): 10557–10564.

Sadeghinezhad, E. *et al*. (2016) 'A comprehensive review on graphene nanofluids: Recent research, development and applications', Energy Conversion and Management. Elsevier Ltd, 111: 466–487.

Sharma, R. and Thakur, R. C. (2017) 'Study of thermodynamic and acoustic behaviour of nicotinic acid in binary aqueous mixtures of D-lactose', AIP Conference Proceedings, 1860.

Sharma, R. and Thakur, R. C. (2018) 'Molecular Interactions of Pyridoxine Hydrochloride in Aqueous Mixed Solutions of D-Glucose, D-Fructose, and D-Lactose at Different Temperatures', Russian Journal of Physical Chemistry A, 92(13): 2685–2692.

Sharma, R. *et al*. (2017) 'Properties of L-ascorbic acid in water and binary aqueous mixtures of D-glucose and D-fructose at different temperatures', Russian Journal of Physical Chemistry A, 91(12): 2389–2396.

Sheshmani, S. and Fashapoyeh, M.A. (2013) 'Suitable Chemical Methods for Preparation of Graphene Oxide , Graphene and Surface Functionalized Graphene Nanosheets', 813–825.

Sonika and Thakur, R. C. (2015) 'Effect of temperature on viscosity B- coefficients of some transition metal chlorides and magnesium chloride in water and in water + methanol mixtures', Research Journal of Pharmaceutical, Biological and Chemical Sciences, 6(1): 664–673.

Sonika *et al*. (2018) 'Molecular Interactions of Transition Metal Chlorides in Water and Water–Ethanol Mixtures at 298–318 K on Viscometric Data', Russian Journal of Physical Chemistry A, 92(13): 2701–2709.

Stankovich, S. *et al*. (2007) 'Synthesis of graphene-based nanosheets via chemical reduction of exfoliated graphite oxide', Carbon, 45(7): 1558–1565.

Su, P. *et al*. (2012) 'An efficient method of producing stable graphene suspensions with less toxicity using dimethyl ketoxime', Carbon. Elsevier Ltd, 50(15): 5351–5358.

Tajik, B. *et al*. (2012) 'Ultrasonic properties of suspensions of TiO_2 and Al_2O_3 nanoparticles in water', Powder Technology, 217: 171–176.

Thakur, R. C. (2016) 'Asian Journal of Chemistry', Asian Journal of Chemistry, 28(12): 2627–2631.

Thakur, R. C. and Sharma, R. (2017) 'Viscometric studies of divalent transition metal sulphates in mixtures of water–diethylene glycol at 298.15–318.15 K', Russian Journal of Physical Chemistry A, 91(9): 1703–1709.

Thakur, R. C. *et al*. (2014) 'Partial molar volumes of aluminium chloride, aluminium sulphate and aluminium nitrate in water-rich binary aqueous mixtures of tetrahydrofuran', Oriental Journal of Chemistry, 30(4): pp. 2037–2041. doi: 10.13005/ojc/300469.

Thakur, R. C.; Sharma, R. and Bala, M. (2016) 'Partial molar volumes of Cobalt nitrate and Nickel nitrate in water and binary aqueous mixtures of DMSO at different temperatures', Journal of Materials and Environmental Science, 7(9): 3415–3420.

Thakur, R. C.; Sharma, R.; Meenakshi, *et al*. (2015) 'Thermodynamic study of copper sulphate and zinc sulphate in water and binary aqueous mixtures of propylene glycol', Oriental Journal of Chemistry, 31(1): 363–369.

Thakur, R.C.; Sharma, R.; Kumar, A.; *et al*. (2015) 'Thermodynamic and transport studies of some aluminium salts in water and binary aqueous mixtures of tetrahydrofuran', Journal of Materials and Environmental Science, 6(5): 1330–1336.

Torrisi, F. *et al*. (2012) 'Ink-Jet Printed Graphene Electronics', ACS Nano, 6(4): 2992–3006.

Vajjha, R.S.; Das, D.K. and Mahagaonkar, B.M. (2009) 'Density measurement of different nanofluids and their comparison with theory', Petroleum Science and Technology, 27(6): 612–624.

Wang, L.; Huang, Y. and Huang, H.J. (2014) 'N-doped graphene@polyaniline nanorod arrays hierarchical structures: Synthesis and enhanced electromagnetic absorption properties', Materials Letters. Elsevier, 124: 89–92.

Wang, Y. *et al*. (2017) 'Fabrication and enhanced electromagnetic wave absorption properties of sandwich-like graphene@NiO@PANI decorated with Ag particles', Synthetic Metals. Elsevier, 229(May): pp. 82–88.

Zhang, H. *et al*. (2017) 'Stability, thermal conductivity, and rheological properties of controlled reduced graphene oxide dispersed nanofluids', Applied Thermal Engineering, 119: 132–139.

Zhu, G. *et al*. (2015) 'CN foam loaded with few-layer graphene nanosheets for high-performance supercapacitor electrodes', Journal of Materials Chemistry A, 3(14): 7591–7599.